MULTIPLICITY CORRELATIONS IN ^{12}C + ^{197}Au

W. Trautmann,[a,*] K. Turzó,[a,+] C. Volant,[b] A.S. Botvina,[a,c]
and the ALADIN-INDRA Collaboration[†]

[a)] Gesellschaft für Schwerionenforschung mbH, D-64291 Darmstadt, Germany
[b)] DAPNIA/SPhN, CEA/Saclay, F-91191 Gif sur Yvette, France
[c)] Institute for Nuclear Research, 117312 Moscow, Russia
[*] Corresponding author, e-mail: w.trautmann@gsi.de
[+] Present address: IKS/KU Leuven, B-3001 Leuven, Belgium
[†] See author list in J. Łukasik *et al.*, contribution to these proceedings.

Abstract

Multiplicity correlations of low-energy pions and energetic protons with intermediate-mass fragments were studied for ^{12}C+^{197}Au collisions at incident energies from 300 to 1800 MeV per nucleon with the 4π INDRA multidetector. The deduced correlation functions $1 + R \approx 1.3$ for inclusive event samples reflect the strong correlations evident from the common impact-parameter dependence of the considered multiplicities. For narrow impact-parameter bins (based on charged-particle multiplicity), the correlation functions are close to unity and do not indicate strong additional correlations. Predictions obtained with intranuclear cascade models coupled to the Statistical Multifragmentation Model are in good agreement with the experimental data.

1 INTRODUCTION

At relativistic bombarding energies, the excitation of Δ isobars represents an important means of energy transfer from the relative motion of the colliding nuclei into other degrees of freedom. Evidence for it is given by the strength of pion production with pion-to-participant ratios of up to 10% at incident energies around 1 GeV per nucleon [1]. The production of pions, at these energies, proceeds predominantly via two-step processes, with the excitation of a Δ resonance in a hard nucleon-nucleon collision being the first step. The excitation of Δ isobars is considered as important also for the heating of the spectator residues via reabsorption or multiple scattering of the Δ or pion [2-5]. The observed multifragmentation of spectator residues and the rise and fall of the fragment multiplicity [6] shows that rather high excitation energies can be reached in these reactions.

Direct experimental evidence for the mechanisms responsible for the heating of the produced spectator systems is difficult to obtain because of the high degree of equilibration that is apparent in their decay [7, 8]. Besides global parameters, such as the spectator mass and excitation energy, little measurable traces of the violent initial reaction stages have been found in the decay patterns. Exceptions exist as, e.g., the sideward enhancement of the fragment emission in proton induced collisions with $E_{\rm p} > 10$ GeV [9, 10], which has been attributed to the kinematics of the primary nucleon-nucleon scatterings [10].

In this work [11], we exploit the capability of the INDRA multidetector [12] to identify low-energy π^+ ($E_\pi \lesssim 35$ MeV) and high-energy protons ($E_{\rm p} \gtrsim 150$ MeV) with the Si-Si(Li)-CsI(Tl) calibration telescopes. We analyze the correlations of the multiplicities of these particles with the multiplicities of intermediate-mass fragments in reactions of ^{12}C + ^{197}Au at incident energies from 300 to 1800 MeV per nucleon which were studied as part of the INDRA experimental program carried out at the GSI Darmstadt.

2 PION DETECTION WITH INDRA

Of the 17 rings of INDRA, the 8 more backward rings, covering the range of polar angles

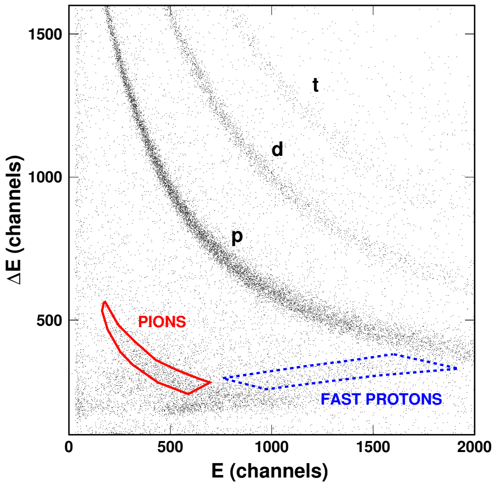

Figure 1: Scatter plot of events in the plane of signals recorded with the 2-mm Si(Li) and the CsI(Tl) detectors of ring 15 ($\langle\theta_{\rm lab}\rangle = 134°$) in the reaction ^{12}C + ^{197}Au at E/A = 1000 MeV. The three lines labelled p, d, t correspond to protons, deuterons and tritons stopped in the CsI(Tl) detector, respectively. The contours indicate the selected regions of stopped π^+ (full line) and of protons punching through the CsI(Tl) detector (dashed).

$45° \leq \theta_{\rm lab} \leq 176°$ and consisting of ionization chambers followed by CsI(Tl) scintillators, are each equipped with a calibration telescope. These telescopes consist of pairs of a 80-μm Si detector and a 2-mm Si(Li) detector which are mounted between the ionization chamber and the CsI(Tl) crystal of one of the modules of a ring [12]. They subtend a small solid angle $\Delta\Omega$ = 13.2 msr per telescope but provide high resolution for the identification of charged particles, as illustrated in Fig. 1.

Besides the three strong groups of the hydrogen isotopes, weaker groups corresponding to pions and to fast protons punching through the CsI(Tl) detector can be recognized. We assume that the branch of stopped pions contains predominantly π^+. The prompt μ^+ from their decay add only a few MeV to the measured energy signal while the decay processes following the capture of negative pions by nuclei of the detector material may cause substantial additional energy deposits in the detector. In the analysis, regions containing stopped π^+ and fast protons were selected that excluded cross-contaminations (Fig. 1). In the case of π^+, these regions extended from $\approx$ 6 MeV to between 30 and 40 MeV of energy deposited in the detectors of which 4 MeV were assigned to the produced μ^+. Slightly larger energy intervals were chosen at the more backward angles because of the reduced interference from punch-through protons. The corresponding ranges of kinetic energies are about 2 MeV up to 35 MeV for π^+ and about 150 MeV to 300 MeV for protons. For the subtraction of the background, caused mainly by reactions in the detector material [13], equivalent regions in the neighborhood of the particle branches were sampled.

3 MULTIPLICITIES AND ANGULAR DISTRIBUTIONS

The observed total multiplicity of charged particles, $M_{\rm c}$, has been chosen as a measure of the violence of the collision which, in first order, is a function of the impact parameter b. Five impact-parameter bins were defined, each with a width $\Delta b = 0.2 \cdot b_0$ where b_0 is

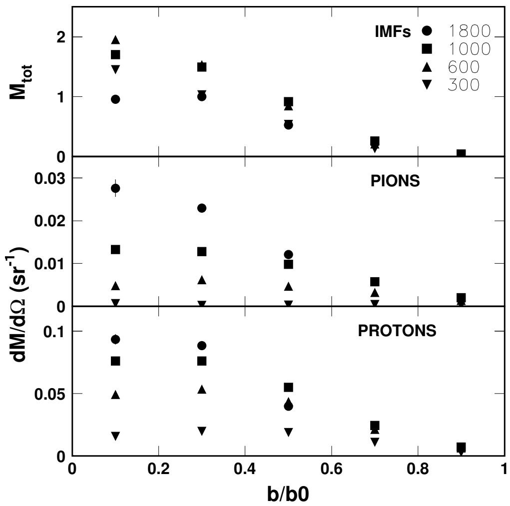

Figure 2: Mean multiplicity of intermediate-mass fragments (top) and mean differential multiplicities $dM/d\Omega$ of stopped π^+ (middle) and of fast protons (bottom), as a function of the relative impact parameter b/b_0 for the reactions ^{12}C + ^{197}Au at E/A = 300, 600, 1000, and 1800 MeV, distinguished by different symbols as indicated. The pion and proton multiplicities are averaged over the angular range $\theta_{\rm lab} \geq 45°$. The data at E/A = 1800 MeV have been evaluated for impact parameters $b \leq 0.6 \cdot b_0$.

the maximum impact parameter contributing at the chosen trigger condition of at least three registered hits in the INDRA detection system.

The mean multiplicities of intermediate-mass fragments with atomic number $3 \leq Z \leq 30$, of stopped π^+, and of fast protons show a general increase with decreasing impact parameter (Fig. 2). The pion and proton multiplicities increase monotonically with the bombarding energy, most clearly visible in the central impact-parameter bins. The energy dependence is different for the fragment multiplicities for which the highest values are reached at 600 and 1000 MeV per nucleon. The maximum is expected for the most central collisions at these energies, according to the impact-parameter dependence observed in the reverse reaction ^{197}Au + ^{12}C [7]. The measured values of below 2, however, are only about half the maximum multiplicities observed in the inverse-kinematics experiments, a difference that is mainly caused by the effective identification threshold for fragments of about 4 MeV per nucleon in the present experiment.

The inclusive angular distributions of low-energy π^+ for 600 and 1000 MeV per nucleon are shown in Fig. 3. They were evaluated for a reduced interval of deposited energy, E = 6 - 27 MeV, which was found free of proton contaminations in all spectra including those at the more forward angles. It corresponds to pion kinetic energies $E_\pi \approx 2$ - 23 MeV. Only the telescope belonging to ring 16 ($\theta_{\rm lab} \approx 149°$) had a high ΔE threshold cutting into the pion branch and was not used for the angular distributions. The uncertainties displayed in this figure are those derived from the fluctuations of the background in the vicinity of the pion branches in the identification maps. These systematic errors are considerably higher at 1000 MeV per nucleon because of the higher background level at this bombarding energy (note that only the statistical errors are displayed in the following figures showing angle-integrated yields).

The angular distributions at the two bombarding energies are very similar, in first order isotropic, with a tendency for a slight rise toward the backward angles. This emission pattern is consistent with multiple rescattering and for absorption processes in the target spectator which is practically at rest in the laboratory. It is in complete contrast to what an extrapolation of the data for high-energy pions would predict. Laue *et al.*, from their measurements for ^{12}C + ^{197}Au at 1000 MeV per nucleon at $\theta_{\rm lab} = 44°$ and 70° and with a threshold $E_\pi > 150$ MeV, have identified a Maxwellian source with temperature T = 68 MeV and velocity $\beta = 0.45$ which permits a good description of their spectra [14]. Its extrapolation to backward angles and low energies leads to an angular distribution which is strongly forward peaked (Fig. 3, dashed line). The effects of rescattering are clearly visible in the angular distribution calculated with the Liège-Intranuclear-Cascade code (see Sect. 5) even though it is still slightly forward peaked (Fig. 3, full line).

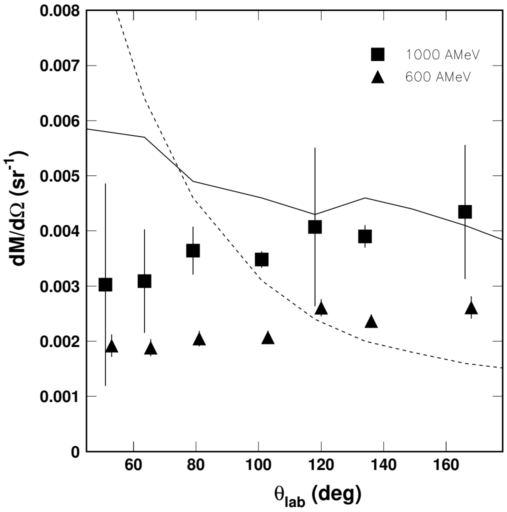

Figure 3: Angular distribution of the inclusive differential multiplicity dM/dΩ of π^+ for the interval of deposited energy E = 6 - 27 MeV for ^{12}C + ^{197}Au at E/A = 600 MeV (triangles) and 1000 MeV (squares). The displayed errors are derived from the fluctuations of the background in the vicinity of the pion branches in the identification maps. The lines represent the corresponding yields for E/A = 1000 MeV predicted by the Liège-Intranuclear-Cascade code (full line) and by a Maxwellian pion source with parameters T = 68 MeV and $\beta = 0.45$ (dashed) which both fit well the π^+ spectra reported in Ref. [14].

4 MULTIPLICITY CORRELATIONS

The multiplicity correlations between the detected low-energy π^+ and intermediate-mass fragments have been expressed in the form of the correlation function

$$1 + R = \frac{\langle M_\pi \cdot M_{\mathrm{IMF}} \rangle}{\langle M_\pi \rangle \cdot \langle M_{\mathrm{IMF}} \rangle} \qquad (1)$$

constructed from the measured coincidences of pions and IMF's and from their single yields [15]. The brackets denote the mean values of the product and individual multiplicities obtained for a given data sample. For orientation, the correlation function is unity ($R = 0$) for uncorrelated emissions and, e.g., has a value $1+R$ $= 4/3$ for the case of a strict proportionality of the two multiplicities and for a homogeneous population within finite multiplicity intervals that start from multiplicity zero.

The correlation functions obtained for pions and fragments and for fast protons and fragments from the inclusive data sets at the four bombarding energies are shown in Fig. 4. For the fragments, the conditions $3 \leq Z \leq 30$ and rapidity $y \leq 0.3$ were introduced so as to select intermediate-mass fragments emitted by the target spectator. The values of $1+R \approx 1.2$ to 1.3 represent strong correlations of the considered multiplicities, as already evident from Fig. 2. The weak variations with the projectile energy are not systematic. No significant result is obtained for the pion-fragment correlation function at 300 MeV per nucleon because the pion multiplicity is very small at this energy (Fig. 2).

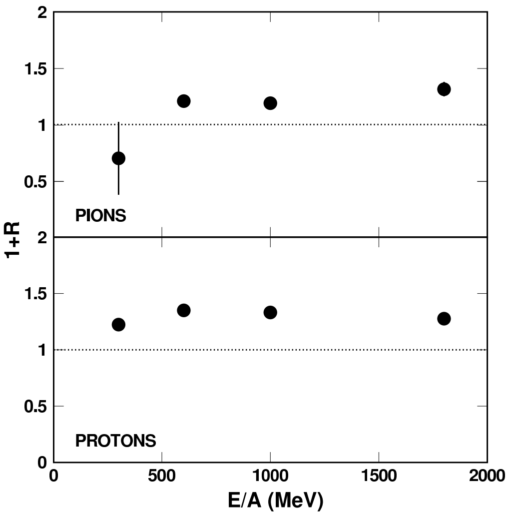

Figure 4: Inclusive multiplicity correlation functions for stopped π^+ and intermediate-mass fragments (top) and fast protons and intermediate-mass fragments (bottom) as a function of the incident energy in ^{12}C + ^{197}Au.

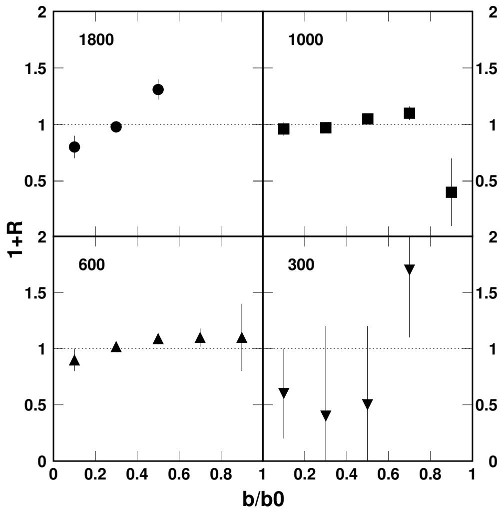

Figure 5: Multiplicity correlation functions for stopped π^+ and intermediate-mass fragments as a function of the relative impact parameter b/b_0 for the reaction ^{12}C + ^{197}Au at E/A = 300, 600, 1000, and 1800 MeV.

The magnitude of the inclusive correlation functions, close to the value derived for the example given above, seems to indicate that they are dominated by the common variation of the considered multiplicities with the impact parameter. More pions and hard nucleon-nucleon scatterings are observed at more central impact parameters. If the contributions of these processes to the energy transfer to the spectator are completely equilibrated at the time of fragment emission, they will influence both, the total charged particle multiplicity that is used for sorting and the multiplicity of fragments. This is what is observed.

In order to test if additional event-wise correlations exist, the correlation functions were also evaluated for the finite impact-parameter bins generated from the total charged-particle multiplicity M_c (Fig. 5). For pions, the statistical uncertainties are large at 300 MeV per nucleon and, at all energies, for the more peripheral collisions for which the multiplicities are small. At 1800 MeV per nucleon, the beam halo introduces additional uncertainties for the event samples at large impact parameter ($b \geq 0.6 \cdot b_0$).

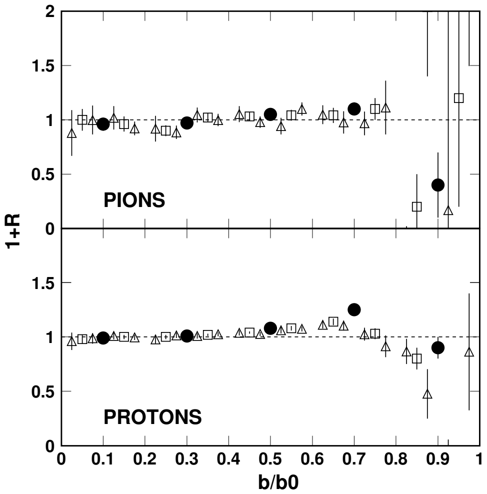

Figure 6: Multiplicity correlation functions for stopped π^+ (top) and fast protons (bottom) with intermediate-mass fragments for the reaction ^{12}C + ^{197}Au at $E/A = 1000$ MeV and for impact-parameter bins of widths $\Delta b/b_0 = 0.05$ (open triangles), 0.1 (open squares), and 0.2 (dots, same as in Fig. 5).

The exclusive correlation functions are, generally, much closer to unity, and most of the observed deviations from unity can be related to residual correlated dependences on impact parameter (M_c) within the chosen finite intervals. At 1800 MeV per nucleon, e.g., the fragment multiplicity decreases with M_c in the most central collisions but increases at $0.4 \leq b/b_0 \leq 0.6$ while the pion multiplicity increases monotonically with M_c. These negative and positive correlations are reflected in the correlation function (Fig. 5, top left). Similarly, the overall tendency towards positive correlations at mid-peripheral impact parameters indicates that here, even within a given bin, the more violent collisions, characterized by a larger number of emitted pions, imply also higher energy deposits and consequently more fragments for the produced spectator systems. These residual correlations should disappear, however, if the widths of the impact-parameter bins are reduced. As demonstrated in Fig. 6, this is also the case, seen most clearly, e.g., for protons in the interval $0.6 \leq b/b_0 \leq 0.8$. The results for the narrower bins are, on average, closer to unity than the value obtained by integrating over the full bin width.

There are weak indications of anticorrelations between pions and fragments that may possibly result from a competition for excitation energy. At 1000 MeV per nucleon, e.g., the individual multiplicities increase with M_c (Fig. 2) which is not reflected in the values for the two most central bins. Choosing the narrowest possible binning (open triangles in Fig. 6), a weighted average of $1 + R = 0.96 \pm 0.03$ is obtained for $b/b_0 \leq 0.4$ from the eight bins covering this interval. This value is practically consistent with unity, i.e. no correlations, but may also be considered as a limit for possible anticorrelations caused by the competition between the emissions of very slow pions and of fragments at the breakup stage.

5 MODEL CALCULATIONS

Two hybrid models were employed for the comparison of the measured multiplicity correlations with theoretical expectations. The Liège relativistic nucleus-nucleus cascade [2] has recently been coupled to a percolation stage used for identifiying excited clusters and nuclear fragments in the nucleon distribution after the cascading stages of the reaction [16, 17]. Their subsequent decay is then followed with the Statistical Multifragmentation Model (SMM) in the version described in Ref. [18]. In the Liège-Intranuclear-Cascade code, the pions are produced through the reactions $NN \rightleftharpoons N\Delta$ and $\Delta \rightleftharpoons \pi N$. The needed cross-sections have been fitted to experimental data when available [3]. A test of the code has been performed by calculating the energy spectra of π^+ emission for the ^{12}C + ^{197}Au reaction at 1000 MeV per nucleon and for the angles $\theta_{\rm lab} = 44°$ and 70° chosen in the KAOS experiment [14]. Nuclear surfaces are sharp in the version used here, and the absolute reaction cross-section has to be estimated. With a normalization with respect to a total reaction cross-section of 3 barns [14], the obtained agreement is very satisfactory (Fig. 7).

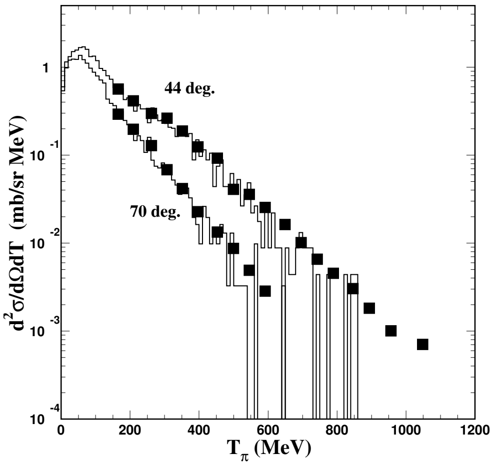

Figure 7: Predictions for π^+ kinetic-energy spectra at $\theta_{\rm lab}$ = 44° and 70° for ^{12}C + ^{197}Au at E/A = 1000 MeV obtained with the Liège-Intranuclear-Cascade (histograms) in comparison with the data from the KAOS experiment (squares, Ref. [14]). The calculations are normalized assuming a total reaction cross section of 3 b.

In a second approach, the intranuclear cascade (INC) model developed in Dubna was used for the simulation of the initial stage of the collision [19, 20]. The INC describes the process of the hadron-nucleon collisions inside the target nucleus. High energy products of these interactions, including pions, are allowed to escape while low energy products are assumed to be trapped by the nuclear potential of the target system. At the end of the cascade, a residue with a certain mass, charge and excitation energy remains which then can be used as input for the statistical description of the fragment production. For this second stage also the Statistical Multifragmentation Model [18] has been used.

The predictions of both models were found to be in very good agreement with the measured correlation functions [11]. No significant difference is caused by the fact that the intermediate configuration of the system is characterized in different ways in the two approaches, by the actual phase space configurations of nucleons in the Liège/percolation model while only the mass and excitation energy of a single spectator source are transferred to the SMM in the Dubna/SMM case. Overall, the observed multiplicity correlations thus confirm the equilibrated nature of the produced spectator configurations prior to their decay.

REFERENCES

[1] P. Senger and H.Stroebele, J.Phys. G25, R59 (1999).

[2] J. Cugnon, Phys. Rev. C **22**, 1885 (1980).

[3] J. Cugnon, T. Mizutani and J. Vandermeulen, Nucl. Phys. **A352**, 505 (1981).

[4] G.E. Brown, Nucl. Phys. **A488**, 689c (1988).

[5] K.B. Morley *et al.*, Phys. Rev. C **54** (1996) 737.

[6] C.A. Ogilvie *et al.*, Phys. Rev. Lett. **67** 1214 (1991).

[7] A. Schüttauf *et al.*, Nucl. Phys. **A607** (1996) 457.

[8] T. Gaitanos, H.H. Wolter, and C. Fuchs, Phys. Lett. B **478**, 79 (2000).

[9] K.H. Tanaka *et al.*, Nucl. Phys. **A583** (1995) 581.

[10] W.-c. Hsi *et al.*, Phys. Rev. C **60** (1999) 034609.

[11] K. Turzó *et al.*, preprint GSI-2003-36, nucl-ex/0402005, Eur. Phys. J. A (in press).

[12] J. Pouthas *et al.*, Nucl. Instr. Meth. in Phys. Res. **A357**, 418 (1995).

[13] V. Avdeichikov *et al.*, Nucl. Instr. Meth. in Phys. Res. **A437**, 424 (1999).

[14] F. Laue *et al.*, Eur. Phys. J. A **9**, 397 (2000).

[15] correlation functions of this kind for thermal photons and intermediate-mass fragments have been reported by C. Agodi *et al.*, in *Proceedings of the XXXIX International Winter Meeting on Nuclear Physics*, Bormio, Italy, 2001, ed. by I. Iori, A. Moroni (Milano, 2001), p. 249.

[16] J. Cugnon and C. Volant, Z. Phys. A **334**, 435 (1989).

[17] D. Doré *et al.*, Phys. Rev. C **63**, 034612 (2001).

[18] J.P. Bondorf *et al.*, Phys. Rep. **257**, 133 (1995).

[19] V.D. Toneev and K.K. Gudima, Nucl. Phys. **A400**, 173c (1983).

[20] A.S. Botvina, A.S. Iljinov, and I.N. Mishustin, Nucl. Phys. **A507**, 649 (1990).